MONITORING OF THE WATER PARTICLE VELOCITY FIELD NEAR THE SEABED UNDER DIFFERENT WAVE AND TIDAL SCENARIOS: A REAL CASE

A.B.M. Khan-Mozahedy[1*], J.J. Munoz-Perez[2] and M.G. Neves[3]

[1]*Bangladesh Water Development Board (BWDB), Wapda bhaban, Motijheel C/A, Dhaka-1000, Bangladesh and Department of Applied Physics, University of Cadiz, Puerto Real Campus, Cadiz-11510, Spain, e-mail:bashar.jrcb@gmail.com*

[2] *Department of Applied Physics, University of Cadiz, Puerto Real Campus, Cadiz-11510, Spain, e-mail:juanjose.munoz@uca.es*

[3]*Laboratorio Nacional de Engenharia Civil (LNEC), Avenida de Brasil 101,1700-066 Lisbon, Portugal, e-mail:gneves@lnec.pt*

ABSTRACT

Monitoring of water particle velocity on the sea bed is crucial to study morphological shore changes in a coast at intermediate and shallow water depth under progressive surface waves and tidal flow current. Therefore, 3-D particle velocity was monitored continuously at the bottom of Santa Maria del Mar (SMM) beach (SW Spain) by means of a single point current meter during 3 weeks in 2007 since August 28. The current meter was placed at 0.45m above the seabed in order to acquire instantaneous velocity. Wave properties (height and period) were taken from the nearby wave buoy and tidal data were taken from a tidal gauge station. Wave-induced bottom particle velocities were obtained during spring and neap tides at a d/L (depth over wave length) parameter ranging from 0.06 to 0.3. Bottom water particle velocity near the seabed ranges from 0 to ± 0.5 m/sec of which about 82% does not exceed 0.2 m/sec during monitoring. Therefore, only 18% of the surveyed water particle velocities exceed the critical Shield parameter of the beach sand (d_{50} = 0.23mm) which is about 0.05-0.2 depending on Reynolds number. Results show that maximum horizontal speed is obviously lower during the slack tide (high or low tide) in comparison with flood tide and ebb tide. Moreover, speed is higher during ebb tide in comparison to adjacent flood tide, with steady wave climate. Finally and among other conclusions, the maximum real values of the bottom current surveyed in SMM, as well as the Shield parameter, substantially coincide with the theoretical estimates calculated for a given wave and tidal climate.

Keywords: *Bottom orbital velocity, Tide, Tidal current, Intermediate water depth, Shield parameter*

1. INTRODUCTION

Wave dissipates its energy to seabed through the water column by means of elliptical orbital motion at intermediate and shallow coastal water depth (Dean and Dalrymple, 1991). Consequently, near shore seabed morphology depends on hydrodynamic velocity fields, i.e., on the ranges of bottom water particle displacements and speeds. Flood-tidal and ebb-tidal flow currents manipulate the wave orbital motions by adding or subtracting itself depending on phases of the both wave and tidal cycles. Water depth becomes reduced during low tide, therefore wave-induced bottom particle velocities and bed shear stresses intensify near the seabed during these tidal moments/phase. Combined interaction of tidal currents and wave-induced orbital motions (Soulsby et al., 1993) causes eccentric oscillation of the bottom particles. Magnitude of the tide-

induced current depends on the tidal prism and tidal currents are low in the Ocean near the coast. Wave-induced bottom water particle velocity and oscillation dispersion depend on progressive surface wave properties (height, period and length) and water level fluctuation (Doering and Baryla, 2002; Wiberg and Sherwood, 2008; Grue et al., 2014), and these velocities and dispersions could be calculated theoretically. These estimates may have similarities with the real case data acquisitions. Tide-induced and wave-induced water particle velocities near the seabed play an important role in the formation of different bedforms and seabed profiles (Enfrink et al., 2006). Any structural intervention in the critical flow field at intermediate water depths may cause sudden change in the prevailing flow pattern resulting new bedforms. Structures installed at the bottom can suffer from this kind of alteration on seabed profile, resulting in structure movements and even on sinking. Two incidences of sinking submerged breakwaters into the Santa Maria der Mar (SMM) sandy seabed during 1998 and 2005 (Medina et al., 2006a) have encouraged the investigation of the bottom particle velocities induced by wave propagation and tidal current. In addition, this study comprises comparison of the real case velocities with theoretical estimates especially water particle velocities and Shield parameters under progressive surface waves alone.

2. STUDY AREA AND EARLIER STUDIES

The monitoring study was conducted at intermediate water depth in SMM, SW Spain during August 28 to September 21, 2007. SMM has a 450 m-long beach with NNW-SSE orientation located on the Gulf of Cadiz, facing the Atlantic Ocean, near the Strait of Gibraltar (Figure 1). The Cadiz coast has mesotidal water level fluctuations, with two high tides a day separated by about 12.42 hours. The tidal range has a medium neap (1st and 3rd quarter of the moon positions) to spring (full and new moon positions) variation ranging from 1.10 m to 3.60 m (Aboitiz et al., 2008) (Figure 3). Wave incidence to the SMM coast generally occurs from west to south-west directions, having significant wave height range 0.4-1.5 m and mean wave period range 4.0-10.0 sec (www.puertos.es, Muñoz-Perez and Medina, 2010). The SMM beach consists of a sandy layer of about 2-3m thick over a rocky platform. Average median sand size (d_{50}) in the emerged beach is about 0.33 mm but sand size substantially decreases (about 0.23 mm) at the submerged beach, close to the already sunk modular breakwater located in between the two heads of the groins (Figure 1). The adjacent Victoria beach presents a rocky platform that is almost horizontal and coincides with sea level at spring low tides (Bernabeu et al., 2002). On the contrary, the rocky stratum of SMM beach is 2-3 m deep and it always remains covered by sand. The beach could be generally classified as eroding because of an average sand loss of about 10,000 m^3 annually (Muñoz-Perez and Medina, 2010). Two groins were built in order to prevent the long-shore loss, but the cross-shore loss still existed and that has

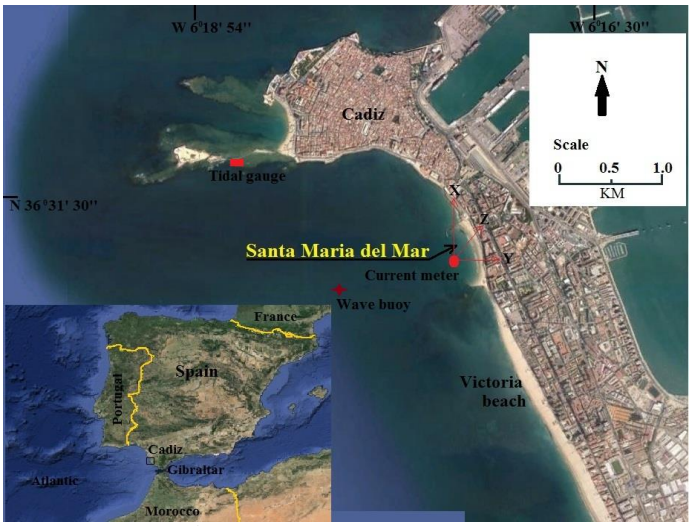

Figure 1: Location of the study area with wave buoy, tidal gauge and current meter

required annual maintenance tasks. In order to avoid this nourishment a submerged breakwater, which was about 400 m long and 2.0 m high, was placed at 3.0 m water depth by joining the two heads of the groins in 1997. After the winter storms and within less than 6 months of installation, a visual inspection found that the breakwater had disappeared (Medina et al., 2006b); the stones had sunk into the sand stratum completely. In order to understand what really happened, some precast concrete modules were placed again and monitored on the same place in 2005. Analysis of data from the monitoring found that the modules also sunk into the overlying sand layer with scouring around the breakwater within 3-6 weeks of deployment. It should be pointed out that, scouring because of wave-structure interaction was suspected as prime cause of sinking in latter occurrence. Bathymetric survey after winter of 2006 found that the scoured area was backfilled with slight accretion (about 0.5-1.0m) shortly after stabilization of the sinking of the submerged modular breakwater (Muñoz-Perez et al., 2015).

3. METHODOLOGY OF THE FIELD CAMPAIGN

3.1 Data Collection

The 3-D velocity data have been acquired by using a single point current meter 'AQUADOPP' (Figure 2A) in this field campaign (more elaborated information may be accessed from http://www.nortekusa.com/usa/products/acoustic-doppler-current-meters). The current meter was placed at 0.45 m above the seabed in between two groins (Figure 1 and 2B). The water depth (varying from about 3.0m to 6.6m, Figure 3) at the current meter position is classified as intermediate considering the prevailing wave length range (about 10m to 30m). However, storm conditions along with high wave length may make the water depth shallow at this monitoring site, depending on the tide level. The AQUADOPP current meter has provided first useful data for the analysis started to be acquired at 11:00 GMT, August 28, 2007 and continued until 11:00 GMT, September 21, 2007. 3-D velocity components (m/sec) were acquired as Northing, Easting and Up-ward directions (Figure 2B) at 10 minute interval, and 60 seconds sample with the frequency of 1 Hz was taken each time. The current meter was anchored on to the seabed by a specially designed parallelepiped structure.

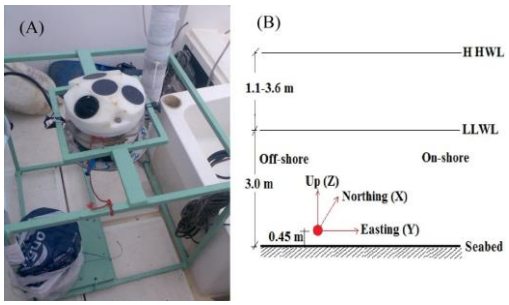

Figure 2: (A) Photograph showing the acoustic doppler current meter 'AQUADOPP' and the anchoring systems ready for deployment (B) Relative position of the current meter above seabed and directions of the 3-D velocity components (HHWL – Higher High Water Level and LLWL – Lower Low Water Level)

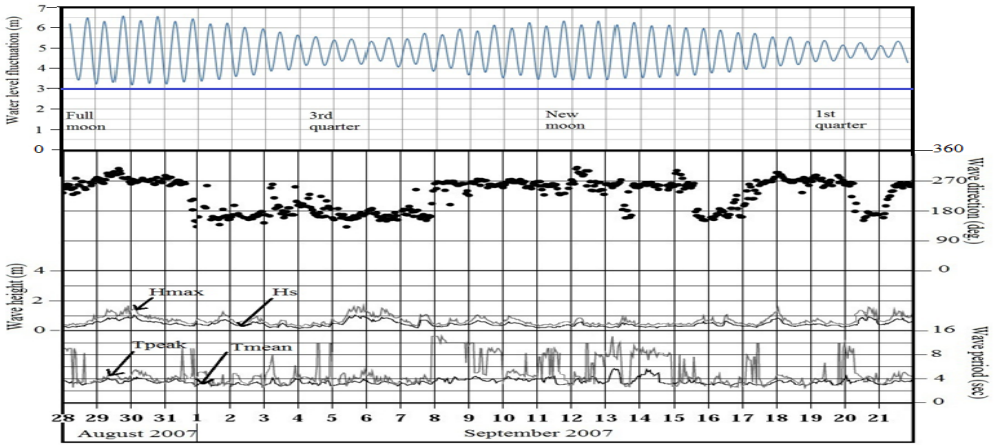

Figure 3: Tidal levels; 3.0 m line represents Lowest Low Water Level and reference water depth, Position of the moon with respect to sun is also mentioned herein and Wave properties (direction of wave incidence- dot points, maximum wave height (H_{max}), significant wave height (H_s), peak period (T_{peak}) and mean period (T_{mean})) (www.puertos.es)

The bottom particle velocity has been acquired as x-component (Northing), u_x; y-component (Easting), u_y and z-component (Up), u_z. Particle speed (U_b) and its horizontal component ($U_{b,hori}$) and vertical component ($U_{b,ver.}$) have been estimated by the following equations.

$$U_{b,hori.} = \sqrt{(u_x^2 + u_y^2)}; U_{b,ver.} = |u_z| \quad (1)$$

$$U_b = \sqrt{(u_x^2 + u_y^2 + u_z^2)} \quad (2)$$

Tidal data has been obtained from the tidal gauge station at Cadiz, Spain. Lower Low Water Level (3.0 meters in the study place along the line joining two heads of the groins, where current meter was placed) serves as reference for the water level in this monitoring study. Wave data (maximum wave height, significant wave height, peak period, mean period and direction of wave incidence) have been collected from a wave buoy at Cadiz, Spain, which is located just off-shore side of the study site (Figure 3).

3.2 Theoretical Background and Data Analysis

If a small amplitude and monochromatic surface wave of period (T) and height (H) propagates from deep water to the shore, according to Linear wave theory the wave length (L) at a water depth (d) can be estimated from the following relationship (Dean and Dalrymple, 1991):

$$L = \frac{gT^2}{2\pi} tanh \frac{2\pi d}{L} \quad (3)$$

Where, g is the gravitational acceleration.

The water particle orbital velocity at 0.45 m above the seabed (Figure 2B), where the velocities are measured, depends on the phases of the surface wave passing over the particle, and this velocity may be ranged from zero to maximum level. According to Linear wave theory, maximum wave orbital velocity ($U_{b,max}$) at this point can be calculated as (Dean and Dalrymple, 1991):

$$U_{b,max} = \frac{\pi H}{T} \cdot \frac{1}{Sinh\{\frac{2\pi(d-0.45)}{L}\}} \quad (4)$$

Friction retards particle velocity significantly at the wave boundary layer close to seabed. So, vertical component of the wave orbital velocity ($U_{ver.}$) becomes zero at the seabed and only horizontal component of the wave orbital velocity ($U_{hori.}$) interacts with the seabed materials.Tidal cycle also creates water particle flow current (U_{tide}) and its magnitude depends on the tidal phases. In the Ocean near the coast, tidal current is negligible, but it may reach appreciable velocity close to the shore at intermediate and shallow water. Tide-induced water particle flow current becomes zero during high tide and low tide (as flow direction changes) and maximum at mean water level during flood tide (flow towards shore) or ebb tide (flow towards sea). So, tide-induced velocity is alternating and it changes direction during every half tidal period. Therefore, bottom water particle velocity at the seabed is the resultant velocity ($U_{b,R}$) of the wave-orbital velocity vector, $U_{b,wave}$ and tide-induced velocity vector, $U_{b,tide}$, given by:

$$U_{b,R} = U_{b,wave} \pm U_{b,tide}\ ;\ U_{b,R} \approx U_{b,wave}\ at\ high\ or\ low\ tide \quad (5)$$

As tide-induced velocity is zero/ negligible during high tide and low tide, it can be assumed that the water particle velocity at high tide or low tide level is induced by wave alone. According to Linear wave theory, amplitude i.e. water particle dispersion (A) of the wave orbital motion at 0.45m above the seabed can be calculated as follow (Dean and Dalrymple, 1991):

$$A = \frac{H}{2} \cdot \frac{1}{Sinh\{\frac{2\pi(d-0.45)}{L}\}} \quad (6)$$

Water particle motion exerts shear stress on the seabed and the level of stress depends on the velocity magnitude and bottom roughness. Friction factor (f_w) for the wave boundary layer at seabed of median sand size (d_{50}), assuming that the seabed is rough, can be calculated as follow (Sumer and Fredsøe, 2002):

$$f_w = 0.04(\frac{A}{k_s})^{-1/4}, \text{ when} \frac{A}{k_s} > 50 \text{ and } k_s = 2.5d_{50} \quad (7)$$

Linear wave theory is applicable at outside of the bottom wave boundary layer. Maximum bed friction velocity (U_{fm}) for the wave boundary layer can be calculated as follow (Sumer and Fredsøe, 2002):

$$U_{fm} = U_{b,max} \cdot \sqrt{\frac{f_w}{2}} \quad (8)$$

Therefore, undisturbed Shield parameter of the seabed can be estimated using the following equation (Sumer and Fredsøe, 2002):

$$\theta = \frac{U_{fm}^2}{g(s-1)d_{50}} \quad (9)$$

Where, s is the specific gravity of the sand.

Shield parameter is the indicator of the initiation of motion of bed materials at the seabed. Maximum Shield parameter of the monitoring site has been calculated using the equation (9) in order to compare the results with maximum Shield parameter calculated using the surveyed velocity data for the same wave properties.

4. RESULTS AND DISCUSSIONS

4.1 3-D Velocity Components of the Bottom Particle Motion

The surveyed three dimensional (3-D) instantaneous velocity components (both magnitude and direction) of the particle motion, which were sampled and measured at 0.45m above the sea bed,

are presented in the Figure 4.There are 3456 samplings measured in each of the three velocity components, corresponding to 25 days of monitoring. Magnitudes and directions of the water particle motion depend on the relative position of the particle with respect to the phase of the propagating surface wave during the instant of measurement. Wave properties (phase, height and period) and tidal properties (range and phase) are linked to the fluctuations of the instantaneous particle velocity.

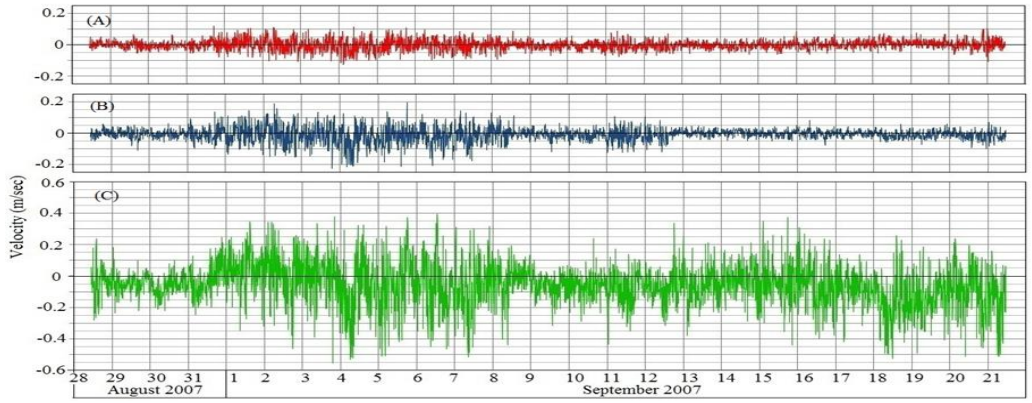

Figure 4: Surveyed bottom particle velocity components; negative magnitude means particle velocity in opposite direction; (A) Northing (x) of the horizontal velocity (B) Easting (y) of the horizontal velocity (C) Vertically up-ward components (z) of the velocity

Water particle velocity profiles (Figure 4) indicate forward and backward oscillatory movement. The x-component of the particle velocity ranges from about 0.1 m/sec (northward) to about -0.1 m/sec (southward) (Figure 4A). The mean of the x-component velocities is almost zero during monitoring period (about 0.0004 m/sec towards north). The y-component of the particle velocity ranges from about 0.15 m/sec (towards shore) to about -0.2 m/sec (towards offshore) (Figure 4B) with a mean 0.008 m/sec towards west (off-shore). Vertical z-component ranges from about 0.35 m/sec (up-ward) to about -0.5 m/sec (down-ward) (Figure 4C) with a mean 0.057 m/sec towards seabed. Vertical components have higher magnitudes during monitoring in compare to horizontal velocity x and y components; posibly because of the influences of nearby debris of the already sunk breakwater. Particle speed and its horizontal and vertical components are calculated using equations 1-2 and are presented in the Figure 5. Horizontal particle speed ranges from 0 to 0.2 m/sec (Figure 5A) with a mean 0.041 m/sec and vertical particle speed ranges from 0 to 0.5 m/sec (Figure 5B) with a mean 0.111 m/sec. Whereas, particle speed ranges from 0 to 0.5 m/sec (Figure 5C) with a mean 0.124 m/sec. About 93.5% of the horizontal particle speeds do not exceed 0.1 m/sec, but in case of vertical particle speeds the distribution are different: about 56% ranges from 0 to 0.1 m/sec, about 28% ranges from 0.1 to 0.2 m/sec and about 11.1% ranges from 0.2 to 0.3 m/sec.

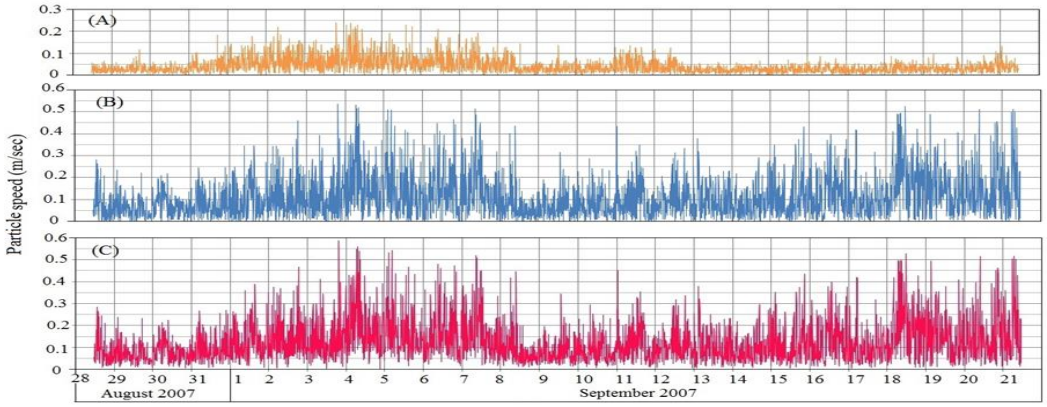

Figure 5: Magnitudes of the bottom water particle oscillatory speeds calculated by equations 1 & 2: (A) Horizontal speeds (B) Vertical speeds and (C) Particle speeds of the 3-D water particle velocity components.

Average wave direction was 270 degree (West) during monotoring period with exception during first week of September, 2007 when wave direction was about 180 degree (South). Maximum wave height has ranged 0.5-1.5 m and significant wave height has ranged 0.4-1.0 m. Peak period has ranged 3-12 sec, while mean period has ranged 3-5 sec. Water depth has ranged from 3.1 m to 6.6 m in the study site (Figure 3). There are higher velocity magnitudes for each of the three components especially horizontal velocities during 1st week of September (Figure 4). The x-component of the horizontal velocity reaches 0.1 m/sec in both directions and while y-component reaches 0.15 m/sec in east direction and 0.2 m/sec in west direction during this period of monitoring. Tide level fluctuations are relatively short (3rd quarter of the moon's position, Figure 3) and wave climate are similar to the days before, with an exception of the direction of wave incidence:wave incidences are mostly from 180 degrees instead of about 270 degrees during most of the time of period of monitoring. Between 18th and 21th of September, there are higher values of vertical velocity magnitudes, reaching -0.5 m/s, the same order of magnitude as measured during the 1st week of September, and higher values of water particle velocity speeds. However, the x and y componentsof velocity, i.e., the horizontal components of the particle speed, do not show the same trend. As for the 1st week of September, tidal level fluctuations are relatively short to (1st quarter of the moon's position, Figure 3) and wave climate are similar to the days before, with an exception of the direction of wave incidence only during 20th to 21th of September.

4.2 Tidal Influences on Wave Orbital Velocity and Bottom Stress

Bottom particle speeds with water level fluctuations at different moon's position are presented in Figure 6 for four different days, corresponding to different tide levels: 29th of August and 05th, 12th and 20th of September. Maximum water particle speeds are considerably lower at full moon's position (29.08.2007) and new moon's position (12.09.2007) when tidal water level fluctuations are maximum and higher at 3rd quarter (05.09.2007) and 1st quarter (20.09.2007) of the moon's positions when tidal water level fluctuations are minimal. On the contrary, maximum horizontal particle speeds are lower at full moon's position (29.08.2007) and 1st quarter (20.09.2007) of the moon's position and higher at 3rd quarter (05.09.2007) of the moon's positions and new moon's position (12.09.2007).Tidal flow currents are negligible during tidal extremes. Although it is difficult to conclude, careful observations find that maximum particle speeds are relatively lower during high or low tides in comparison to the adjacent flood or ebb tidal flow with similar wave climates. For instance, maximum particle speed is about 0.15 m/sec during high tide (29.08.2007

at 7:00 hour) while it is about 0.17 m/sec during preceding flood tidal flow (29.08.2007 at 3:30 hour).Tidal flow currents at either flood or ebb tidal conditions are usually horizontal and unidirectional in nature (either towards shore during flood tidal flow or alternatively towards off-shore during ebb tidal flow). Similar to the particle speeds, it seems that maximum horizontal particle speeds are also lower during high tide and low tide in comparison with the adjacent flood tide and ebb tide at few instances (Figure 6).

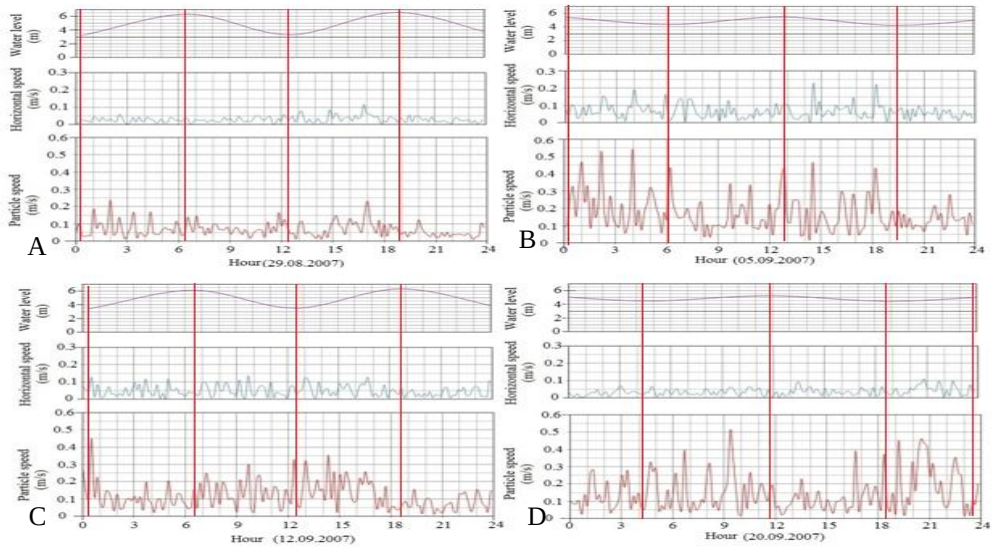

Figure 6: Influence of tidal water level fluctuations in water particle speed and its horizontal component at different moon positions; A-Full moon, B- 3rd quarter, C- New moonand D- 1st quarter.

Tidal water level fluctuations and corresponding bottom wave orbital velocities is presented in Table 1. Analysing the values, it is found that maximum wave orbital velocities (considering negligible tidal flow currents during tidal extremes) and their horizontal components are lower during high tide in comparison to the adjacent low tide with similar wave climates (column 3-4). Maximum water particle speed and its horizontal component at high or low tides of different moon positions are calculated from the current meter data record files (Figure 6) and presented in the 3rd and 4th column of the Table 1. Corresponding wave properties properties (Maximum wave height and peak period) are also determined from the wave data using standard analysis either in the frequency and time domain (Figure 3) and presented in the 5th and 6th column. Theoretical maximum bottom particle speeds for the given wave properties and water level fluctuations (7th column) are calculated using equation 5 and presented in the 8th column. Maximum horizontal particle speeds (column 4) during the 4 days of the four moon's position are about 10-35% of the maximum particle speeds (column 3). Maximum particle speeds (0.16-0.18 m/sec during low tide and 0.12-0.18 m/sec during high tide) surveyed in the current meter during full moon position (29.08.2007) do not match with the calculated theoretically values (0.62-1.09 m/sec during low tide and 0.31-0.39 m/sec during high tide); differences are large considering the given wave climate (wave height 0.8-1.3 m, period 4-5 sec, Figure 3).On contrary, surveyed maximum particle speeds in 3rd quarter (0.44 m/sec during low tide and 0.32-0.43 m/sec during high tide) and in new moon position (0.33-0.45 m/sec during low tide and 0.17-0.25 m/sec during high tide) resemblance with the theoretically calculated values. Two values (one during low and another during high tide) during 1st quarter of the moon position (20.09.2007) are in congruence with

theoretical values while other two values have moderate difference. According to Table 1, higher wave heights and lower water depths have larger values of the bottom particle orbital speeds.

Wave-induced bottom stress at the seabed is represented by the Shield parameter. Measured maximum Shield parameter of the monitoring site have been calculated (equations 7-10) using the calculated maximum particle speeds (column 3) and the given wave climates (column 5-7) and the results are presented in the column 9 of the Table 1. Similarly theoretical maximum Shield parameters (using the theoretical maximum particle speeds-column 8 and the given wave climates-column 5-7) are calculated for comparison and presented in the column 10.Wave orbital velocity at the seabed largely depends on the water depth (eq.5): as expected, considerably lower particle speeds are surveyed during high tide compared to low tide at lower water depth. Highest values of

Table 1: Comparisons between measured and theoretically calculated maximum particle speeds and shield parameters because of wave propagation at current meter position during different tidal extremes

Moon position (1)	**Tidal level (2)**	**Measured max. particle speed (m/sec)(3)**	**Measured max. hor. particle speed(m/sec) (4)**	**Max. wave height, H_{max} (m)(5)**	**Peak period, T_{peak}(sec) (6)**	**Water depth, d (m) (7)**	**Theoretical max. particle speed(m/sec)(8)**	**Calculated Shield parameter (9)**	**Theoretical Shield parameter (10)**
Full moon (29.08.07)	Low	0.18	0.05	0.8	4	3.2	0.62	0.04	0.42
	High	0.14	0.04	0.9	4	6.3	0.31	0.03	0.12
	Low	0.16	0.07	1.3	5	3.3	1.09	0.02	1.07
	High	0.12	0.05	1.2	4	6.5	0.39	0.02	0.19
3rd quarter (05.09.07)	High	0.32	0.10	0.8	4	5.4	0.34	0.13	0.15
	Low	0.44	0.16	0.7	5	4.3	0.46	0.21	0.23
	High	0.43	0.11	1.2	4	5.4	0.51	0.21	0.3
	Low	0.44	0.21	1.3	4	4.2	0.75	0.2	0.59
New moon (12.09.07)	Low	0.45	0.12	0.6	5	3.4	0.49	0.22	0.26
	High	0.25	0.10	0.8	4	6.1	0.27	0.08	0.10
	Low	0.33	0.12	0.4	6	3.5	0.34	0.12	0.13
	High	0.17	0.06	0.4	8	6.3	0.24	0.03	0.07
1st quarter (20.09.07)	Low	0.33	0.06	0.5	9	4.5	0.38	0.11	0.14
	High	0.20	0.05	1.3	4	5.2	0.58	0.04	0.37
	Low	0.45	0.06	1.4	4	4.4	0.77	0.21	0.61
	High	0.20	0.07	0.7	4	5.1	0.32	0.05	0.13

maximum measured particle speed, horizontal particle speed and Shields parameter were obtained from measured data for 3rd quarter (05.09.2007), contrarily of it was expected theoretically. Depending on the Reynolds number, critical Shield parameter for initiation of bed materials in marine environments ranges from 0.05 to 0.2 (Sumer and Fredsøe, 2002). Considering threshold level of the critical Shield parameter (0.05), water particle velocity which exceeds 0.2 m/sec may produce motion in the bed materials for the given wave climates. Particle's horizontal speed may not bring motion in bed materials alone as this speed rarely exceed the speed limit of 0.2 m/sec. But according to analysis, about 18% of the bottom water particle velocity in the monitoring site causes movement of the bed materials in the seabed. Although particle horizontal speed do not bring bed materials into motion, this speeds may impart net transport of the suspended materials towards off-shore at a slow pace. Comparisons of the surveyed maximum water particle speeds and corresponding Shield parameters with the theoretically calculated values during different tidal extremes are presented in the Figure 7. Measured values will be slightly lower than the theoretically calculated values in any case depending on the efficiency of the system. Measured

wave orbital speeds and Shield parameters in the monitoring are calculated based on the maximum surveyed velocity magnitudes, but these surveyed values may not be maximum at the monitoring instance. Therefore, surveyed maximum particle speeds and corresponding Shield parameters are in accordance with the theoretically calculated values except for 4 instances of low tide and 1 instance of high tide out of total 16 instances. These differences could be explained by the possibility that the current meter missed the maximum magnitudes in those 5 instances. However, measured maximum wave orbital speeds at 45 cm above the seabed are similar to and slightly lower than the theoretically calculated values. Similarly measured maximum Shield parameters are in accordance with the theoretically calculated values for a given wave climate and depth.

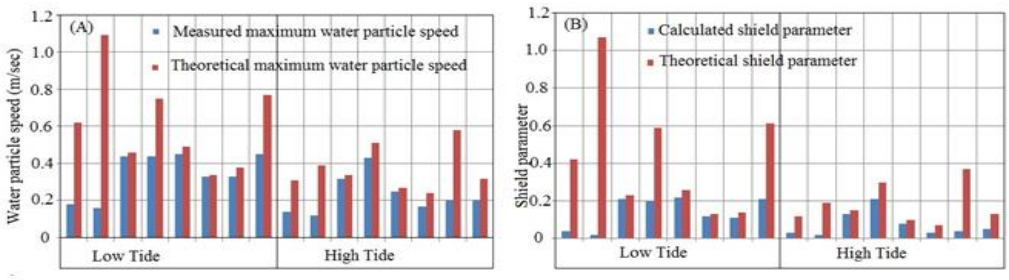

Figure 7: (A) Comparison of the surveyed maximum water particle speeds with the theoretically achievable values during different tidal extremes (B) Comparison of the calculated shield parameters of the seabed based on the surveyed maximum water particle speeds with the theoretically calculated values during the different tidal extremes.

5. CONCLUSION

Bottom particle velocity field under combined mesotidal flow and progressive surface wave propagation has been evaluated at intermediate and shallow water depth in this monitoring study at SMM, Spain, based on measurements made with a current meter deployed 0.45m from the bed. The following conclusions can be made based on the results of the study:

1. Mean horizontal speed denotes that net movement of the particles directs seawards at a mean speed of 0.008 m/sec.
2. Tidal range has a significant role in measuring water depth which influenced directly the particle speed at intermediate depth; tidal flow velocity cannot be separated from wave-induced velocity effectively in this water depth, however it seems that maximum horizontal particle speeds are lower during high tide and low tide when comparing with flood tide and ebb tide at some instances.
3. Considering critical value of the Shield parameter (0.05-0.2, depending on Reynolds number), critical value of the particle speed is about 0.2 m/sec for initiation of motion in the seabed material of the monitoring site. Water particle speed ranges up to 0.5 m/sec and about 18% of the particle speeds may cause scouring in the seabed.
4. Although, bottom particle speeds exceed critical level of the Shield parameter, the seabed maintains equilibrium because of low horizontal speeds. Therefore, any structural intervention on this seabed may change the magnitude and direction of the horizontal velocity components and could result in extensive scouring and sinking close to the structure.
5. Wave-induced particle speed depends on the instantaneous phase of the progressive surface wave and its properties (height, period and direction); non-tidal wave-induced maximum bottom water particle speeds are in congruence of the theoretical estimates especially during 3rdquarter and new moon positions.

REFERENCES

Aboitiz, A., Tejedor, B., Munoz, J.J., Abarca, J.M., 2008. Relation between daily variations in sea level and meteorological forcing in Sancti Petri channel (SW Spain).Cienc. Mar. 34, pp.491-501

Bernabeu-Tello, A., Muñoz-Pérez, J.J., & Medina-Santamaría, R. (2002). Influence of a rocky platform in the profile morphology: Victoria Beach, Cadiz (Spain). Ciencias Marinas, 28(2), pp. 181-192

Dean, R.G., Dalrymple, R.A., 1991. Water wave mechanics for Engineers and Scientists. World Scientific, Singapore

Dalyander, P.S., Butman, B., Sherwood, C.R., Signell, R.P., Wilkin, J.L., 2013. Characterizing wave- and current- induced bottom shear stress: U.S. middle Atlantic continental shelf. Continental Shelf Research 52, pp. 73-86

Doering, J.C., Baryla, A.J., 2002. An investigation of the velocity field under regular and irregular waves over a sand beach. Coastal Engineering 44, pp. 275-300

Elfrink, B., Hanes, D.M., Ruessink, B.G., 2006. Parameterization and simulation of near bed orbital velocities under irregular waves in shallow water. Coastal Engineering 53, pp. 915-927

Grue, J., Kolaas, J., Jensen, A., 2014. Velocity fields in breaking-limited waves on finite depth. European Journal of Mechanics B/Fluids 47, pp.97-107

Kagan, B. A., Alvarez, O., Izquierdo, A., 2005. Weak wind-wave/tide interaction over fixed and moveable bottoms: a formulation and some preliminary results. Continental Shelf Research 25(7), 753-773.

Myrhaug, D., Slaattelid, O.H., Lambrakos, K.F., 1998. Seabed shear stresses under random waves: predictions vs estimates from field measurements. Ocean Engineering 25 (10), pp. 907-916

Medina, J.R., J.J. Muñoz-Perez, G. Gomez-Pina, 2006a. Transmission and Reflection of Modular Detached Breakwaters. Coastal Eng. Conf. (ASCE) 30 (5), pp.4350-4361

Medina, J., Muñoz-Perez, J. J., Tejedor, B., Gomez Pina, G., Fages, L., 2006b. Actuacion experimental con diques modulares en Santa Maria del Mar. Redes neuronales, socavacion y licuefaccion de arenas. II Congreso Nacional de la AsociacionTecnica de Puertos y Costas, pp.301-322

Muñoz-Perez, J.J., Medina, R., 2010. Comparison of long-, medium- and short-term variations of beach profiles with and without submerged geological control. Coastal Engineering 57, pp.241-251

Muñoz-Perez, JJ, Roman-Sierra, J, Navarro-Pons, M., Neves, M.G., del Campo, J.M., 2014. Comments on "Confirmation of beach accretion by grain-size trend analysis: Camposoto beach, Cádiz, SW Spain" by E. Poizot et al.(2013). Geo-Marine Letters 34 (1), 75-78

Muñoz-Perez, J.J., Khan-Mozahedy, A.B.M., Neves, M.G., Tejedor, B., del Campo, J.M., Negro, V.,2015. "Sinking of concrete modules into a sandy seabed: a case study". Coastal Engineering, in press

Román-Sierra, J., Muñoz-Perez, J.J., Navarro-Pons, M., 2013. Influence of sieving time on the efficiency and accuracy of grain-size analysis of beach and dune sands. Sedimentology 60, pp.1484 –1497

Román-Sierra, J., Muñoz-Perez, J.J., M. Navarro-Pons, 2014. Beach nourishment effects on sand porosity variability, Coastal Engineering 83, pp 221-232

Sumer, B.M., Fredsøe, J., 2002. The mechanics of scour in the marine environment, Advanced series of ocean engineering, vol.17. World Scientific, Singapore

Soulsby, R.L., 1987. Calculating bottom orbital velocity beneath waves. Coastal Engineering 11, pp. 371-380

Soulsby, R.L., Hamm, L., Klopman, G., Myrhaug, D., Simons, R.R., Thomas, G.P., 1993. Wave-current interaction within and outside bottom boundary layer. Coastal Engineering 21, pp. 41-69

Wiberg, P.L., Sherwood, C.R., 2008. Calculating wave-generated bottom orbital velocities from surface-wave parameters. Computers & Geosciences 34, pp. 1243-1262